HIGH STRAIN RATE DEFORMATION BEHAVIOR OF AL-MG ALLOYS

T. Masuda[1], T. Kobayashi[2] and H. Toda[2]

[1]Graduate Student, Graduate School of Toyohashi University of Technology
[2]Department of Production Systems Engineering, Toyohashi University of Technology,
Toyohashi-city, AICHI, 441-8580, Japan

ABSTRACT

The aim of the present study is to characterize the strain rate dependency and the microstructural change behavior of Al-Mg series alloys over a wide range of strain rate. Impact tensile tests are carried out using a split-Hopkinson bar apparatus and servo hydraulic testing machine. SEM observation is made to analyze the microstructural changes of fracture surface. Al-Mg alloys show an increase in 0.2% proof stress, ultimate tensile strength, elongation, reduction of area and work hardening exponent with increasing strain rate. Although strain rate dependency of the stress and work hardening exponent are negligible up to the strain rate of approximately $10^2 s^{-1}$, the extent of rate sensitivity appears to increase from this strain rate. The elongation and reduction of area show linear increases with increasing strain rate. Although fracture surfaces mainly exhibit the shear type dimple pattern under the low strain rates, ordinary equiaxed dimple fracture is observed under the high strain rates.

KEYWORDS

Hopkinson bar, strain rate dependency, Al-Mg series alloys, impact tensile test, SEM, fracture surface, dimple, impact stress-strain curve

INTRODUCTION

The dynamic deformation behaviors of materials have become increasingly important in many applications related to the design especially in the field of transportation industry such as automobiles. Because Al-Mg series alloy has superior mechanical properties such as a high strength/weight ratio, good corrosion resistance and deformability, it is considered for many advanced applications where the structural components are subjected to dynamic loading. In order to optimize deformation and fracture performance of this alloy under the high strain rates, it is necessary to understand the dynamic deformation mechanisms [1].
It is recognized that materials often respond in different ways to high strain rate loading as compared to low strain rate loading. As strain rate is increased from static to dynamic, it results in an increase of the strength with increasing strain rate. Further, the flow stress of a material depends not only on the strain and strain rate but also on its microstructure especially at the dislocation level. In order to combine the micromechanisms of deformation and macroscopic constitutive relationships, there is a need to understand the microstructural changes which take place during deformation [2,3]. Therefore, it is the purpose of this work to study the

impact response of commercial Al-Mg series alloys deformed in the stain rate range of 10^{-4} to $10^{4}s^{-1}$ and, further, to investigate the microstructural changes.

MATERIALS AND EXPERIMENTS

Two kinds of work hardening aluminum alloys used in this investigation are 5052-H112 and 5083-H112 alloys. The chemical compositions are listed in Table1. Geometry and nominal dimensions of the tensile specimens are given in Fig.1 [4,5] and Fig. 2. All specimens used in static tensile, dynamic servo hydraulic tensile and dynamic split-Hopkinson bar tests have the same gage length and diameter.

TABLE 1

CHEMICAL COMPOSITIONS OF SAMPLES USED

(mass%)

	Si	Fe	Cu	Mn	Mg	Cr	Zn	Ti	Al
5052-H112	0.09	0.25	0.03	0.04	2.50	0.19	0.01	0.01	bal.
5083-H112	0.14	0.20	0.03	0.65	4.64	0.11	-	0.02	bal.

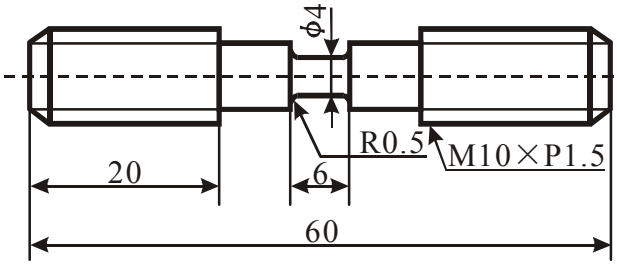

Figure 1: Geometry of a specimen in the static and dynamic tensile tests.

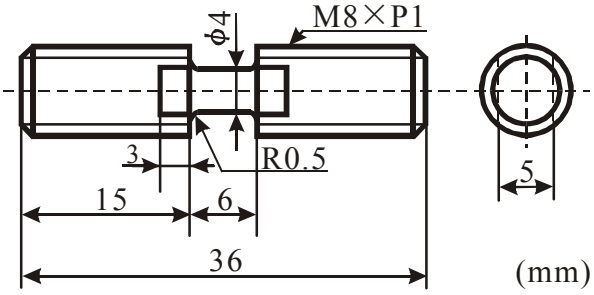

Figure 2: Geometry of a specimen in the split-Hopkinson bar test.

Static tensile experiments were carried out using the Instron testing machine. Intermediate rate tests were made on a servo-controlled hydraulic testing machine over a range of strain rates approximately from 10^{-1} up to $10^{3}s^{-1}$. The split-Hopkinson bar test was conducted for strain rate exceeding approximately $10^{3}s^{-1}$ [6,7]. All of tests were conducted at room temperature. Fracture surfaces of the tested specimens were observed with a scanning electron microscope.

RESULTS AND DISCUSSION

Stress-Strain Curves over a Wide Range of Strain Rates

Figures 3 and 4 show the typical stress-strain curves at four strain rates (4×10^{-4}, 10^{-1}, 1×10^{3} and $3\times10^{3}s^{-1}$) for the 5052-H112 and 5083-H112 alloys, respectively. In comparison with the result of the static loading condition, the 0.2% proof stress, ultimate tensile strength and elongation showed increases with increasing strain rate. Stress-strain curves showed a three-step process in which there were an initial elastic deformation region, uniform plastic deformation region until the maximum stress, then unstable deformation to the failure. In the static loading, the fracture occurred immediately when the stress reached the maximum stress. However, the flow stress decreased gradually at the high strain rate after the maximum stress. In the case of the dynamic tensile test using the split-Hopkinson bar apparatus, the stress-strain curves could be recorded exactly from the initial elastic deformation to the final fracture as compared to the other techniques.

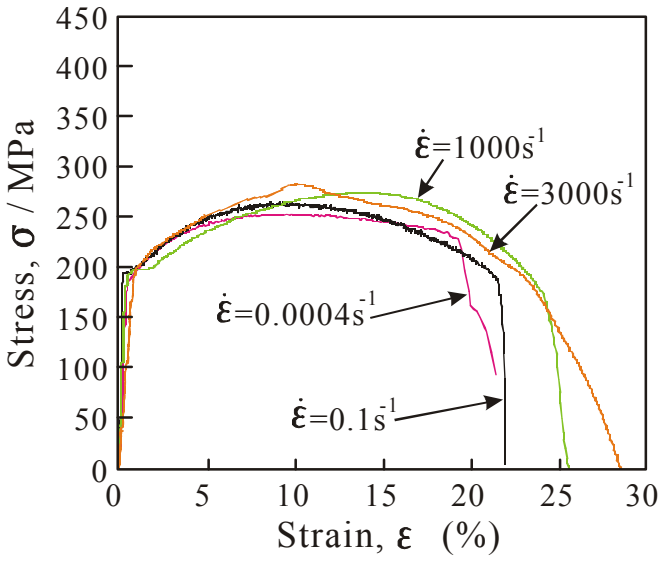

Figure 3: Typical stress-strain curves of the 5052-H112 alloy at various strain rates.

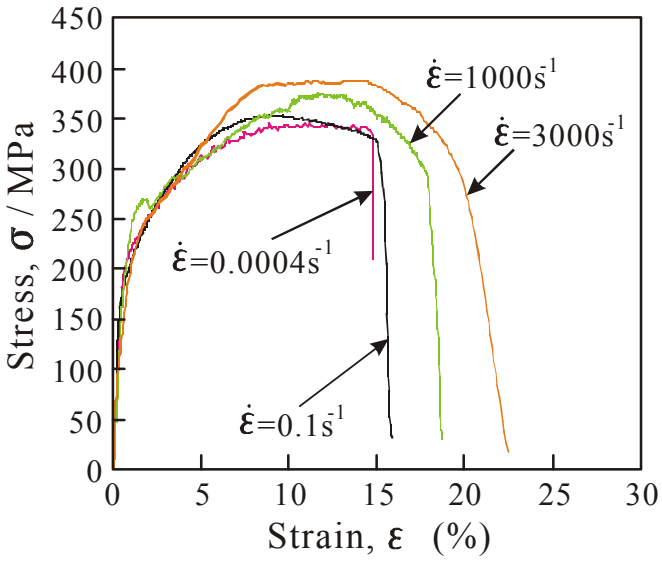

Figure 4: Typical stress-strain curves of the 5083-H112 alloy at various strain rates.

Strain Rate Dependency of Tensile Properties

Figures 5 and 6 show the 0.2% proof stress and ultimate tensile strength as a function of strain rate in the 5052-H112 and 5083-H112 alloys. Although strain rate sensitivity of the ultimate tensile strength is negligible up to the strain rate of approximately $10^2 s^{-1}$, the degree of rate sensitivity appears to increase for the higher strain rates. Tanimura, *et al.* [8] reported that the aluminum alloys containing magnesium solute atoms showed the negative strain rate dependency at intermediate strain rate. However, the negative strain rate dependency could be scarcely recognized in this study. The 5083-H112 alloy shows higher strength than the 5052-H112 alloy. Under the same strain rate range, the 5083-H112 alloy showed a larger strain rate dependency compared with the 5052-H112 alloy. While the 5052-H112 alloy showed an increase in the ultimate tensile strength of approximately 31MPa in the strain rate range of 4×10^{-4} to $3\times10^{3} s^{-1}$, that of the 5083-H112 alloy was approximately 43MPa.

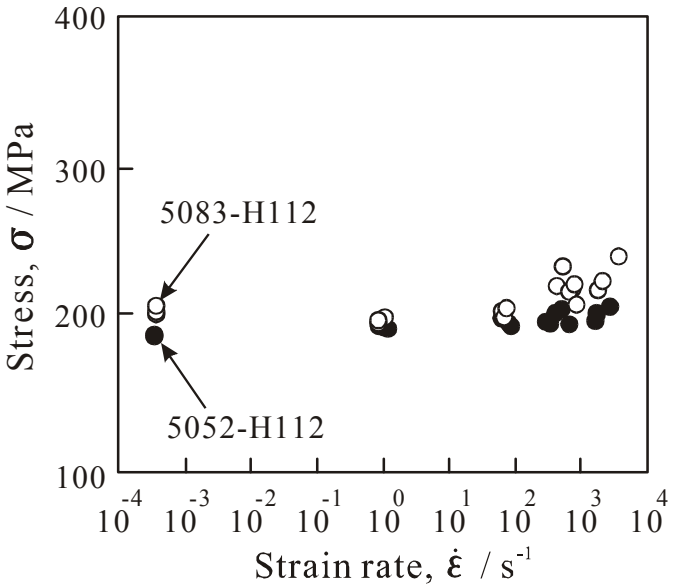

Figure 5: Variation of 0.2% proof stress with nominal strain rate.

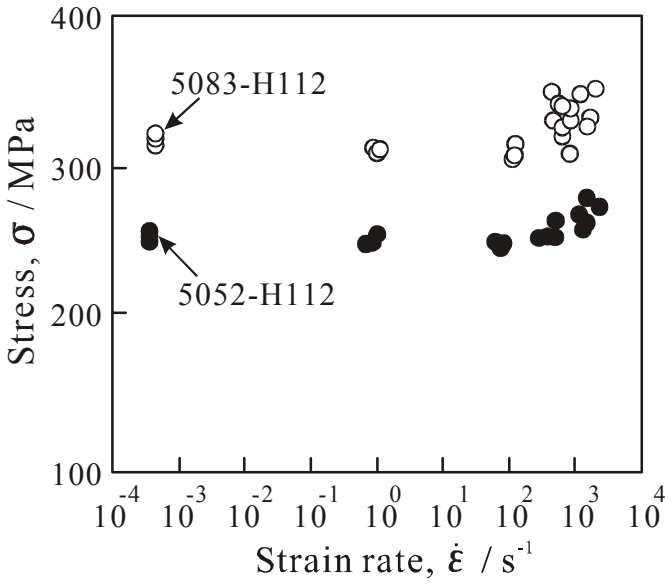

Figure 6: Variation of ultimate tensile strength with nominal strain rate.

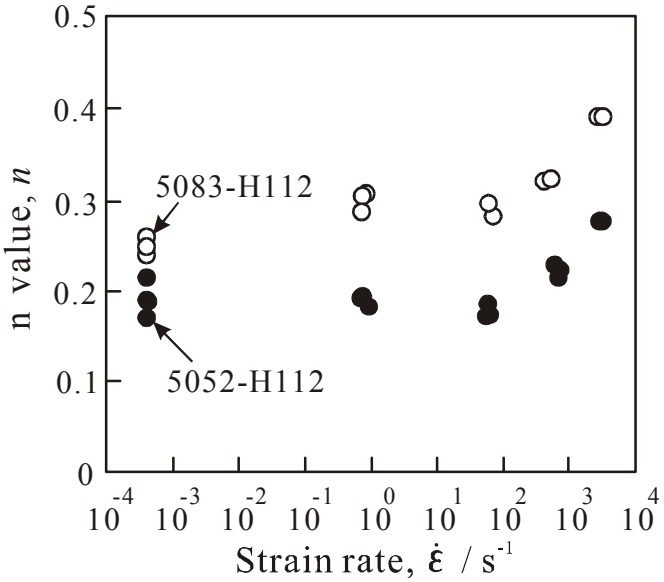

Figure 7: Variation of strain hardening exponent with nominal strain rate.

Figure 7 presents the variation of strain hardening exponent with the strain rate. The strain hardening exponent showed a similar strain rate dependency with the 0.2% proof stress and ultimate tensile strength. However, the increase in the strain hardening exponent was kept constant up to a strain rate of approximately $10^2 s^{-1}$. The 5083-H112 alloy contains approximately twice magnesium element as compared to the 5052-H112 alloy: however strain rate dependency was similar.

Figures 8 and 9 present the variation of elongation and reduction of area with strain rate. The elongation and reduction of area increase linearly with increasing strain rate. Although the strain rate dependency in elongation and reduction of area is negligible up to the strain rate of approximately $10^0 s^{-1}$, the degree of rate sensitivity appears to increase rapidly for the higher strain rates.

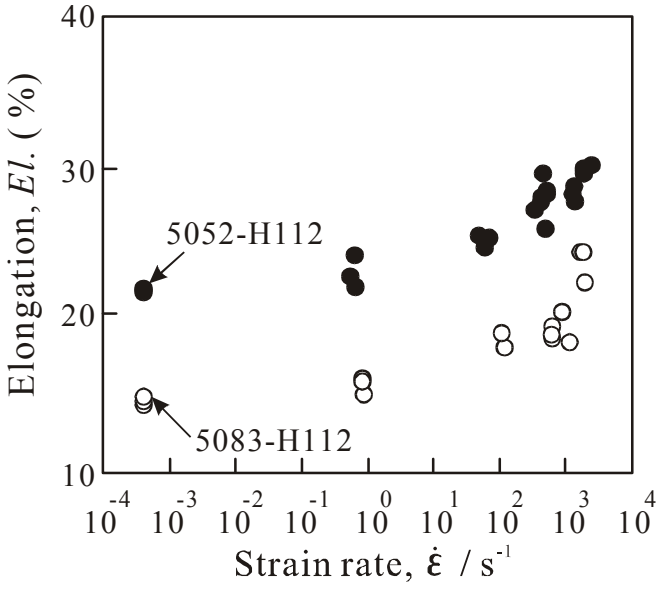

Figure 8: Variation of elongation with nominal strain rate.

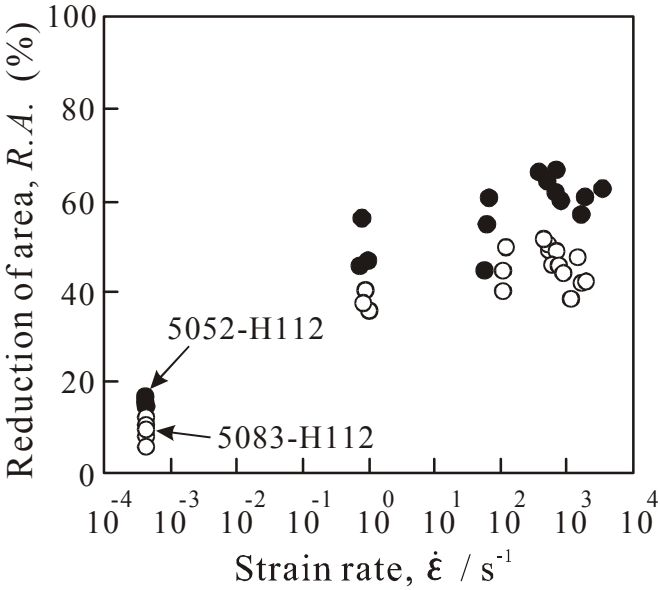

Figure 9: Variation of reduction of area with nominal strain rate.

Effect of the Strain Rate on Fracture Surface and Structure

Figure10 shows the SEM micrographs of the fracture surfaces of the 5052-H112 and 5083-H112 alloys at various strain rates. Both Al-Mg series alloys provide the flat surfaces at static load conditions. However, the fracture occurred by a combination of two different dimple sizes at higher strain rates, one of which is approximately 10 μm and the other is several micrometer in the case of 5083-H112 alloy having higher magnesium content. The fracture surface of low magnesium 5083-H112 alloy is mainly dominated by dimples of approximately 20 μm in diameter. Although the fracture surfaces mainly exhibited the shear type dimple pattern under low strain rates, ordinary equiaxed dimple fracture surfaces were observed under high strain rates. The specimen was largely necked at high strain rate. In both materials, the dimple size and depth increased with the strain rate.

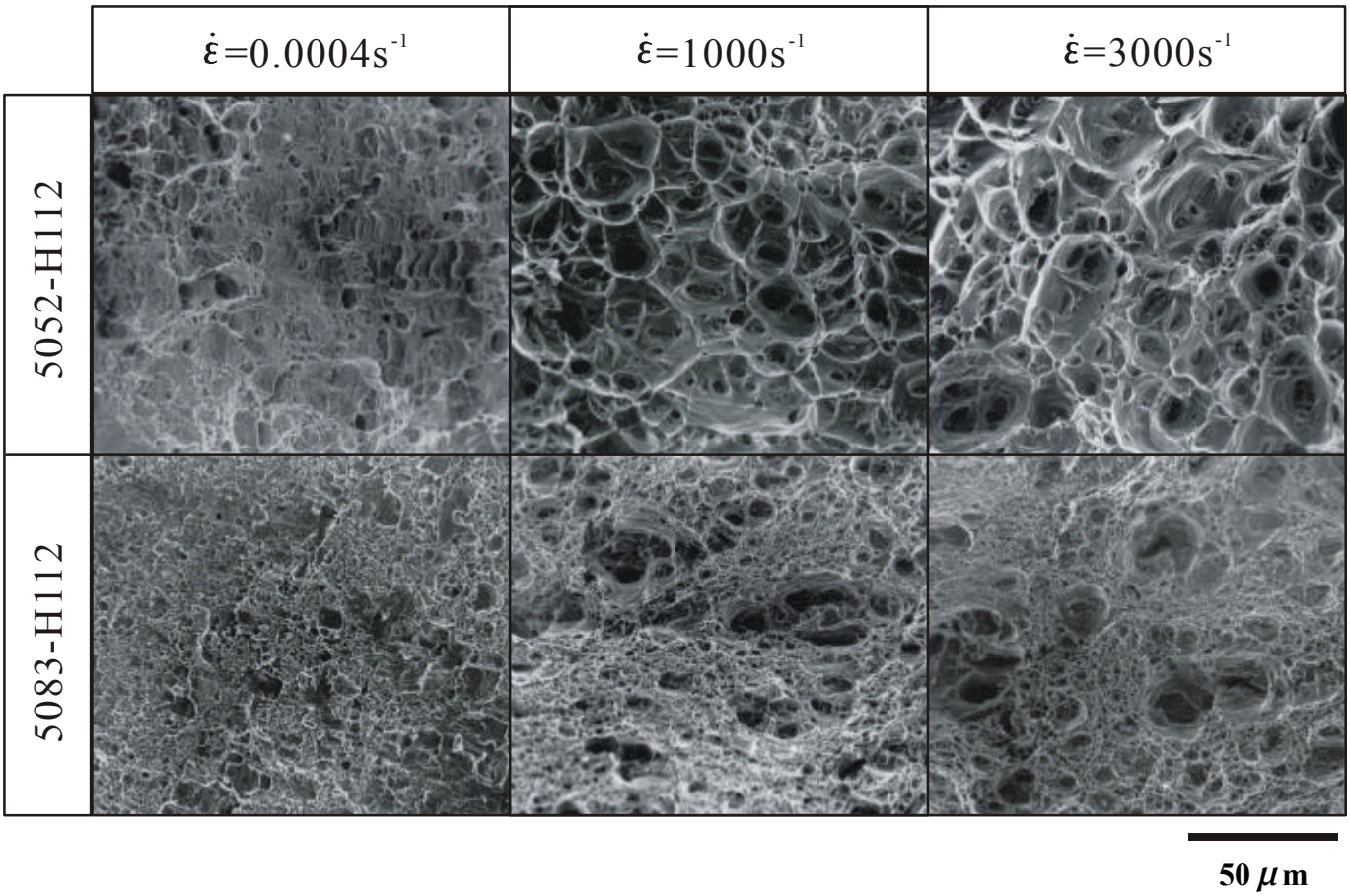

Figure 10: SEM micrographs of fracture surfaces at various strain rates.

CONCLUSIONS

The effect of strain rate on mechanical properties and microstructural changes in 5052-H112 and 5083-H112 aluminum alloys were examined over a wide range of strain rate. The following conclusions could be drawn.

1. The strain rate dependencies of two kinds of Al-Mg series alloys were very sensitive at high strain rate. As the strain rate increased, 0.2% proof stress and ultimate tensile strength increased. Under the same strain rate conditions, the 5083-H112 alloy showed more clear increase in strength than the 5052-H112 alloy.

2. The strain hardening exponent can be seen to increase with increasing strain rate. Strain hardening exponent showed similar degree of strain rate dependency with the 0.2% proof stress and ultimate tensile strength. However, the increasing rate of the strain hardening exponent was constant up to the strain rate of approximately 10^2s^{-1} for both materials.

3. The elongation and reduction of area increased markedly with increasing strain rate, and these dependencies were linear. Although strain rate dependencies in the elongation and reduction of area were negligible up to the strain rate of approximately $10^0 s^{-1}$, the degree of rate sensitivity appears to increase rapidly for the higher strain rates.

4. Although the fracture surfaces mainly exhibited the shear type dimple pattern under the low strain rates, ordinary equiaxed dimple fracture surfaces were observed under the high strain rates. The specimen was remarkably necked at the high strain rate. In both materials, the dimple size and depth increased as the strain rate increased.

REFERENCES

1. Nicholas, T. (1981) *Exp. Mech*., 21, 177.
2. Lindholm, U. S. (1964) *J. Mech, Phys. Solids*, 12, 317.
3. Perzyna, P. (1974). In: *Mechanical Properties at High Rates of Strain,* pp. 138-153, Harding, J.(Ed). Inst. Phys., Oxford.
4. Sugiura, N., Kobayashi, T., Yamamoto, I., Nishido, S. and Hayashi, K. (1995) *J. J. Inst. Light Met.,* 45, 633.
5. Sun, Z. M., Kobayashi, T., Fukunasu, H., Yamanoto, I. and Shibue, K. (1998) *Metall. Mater. Trans.* A, 29A, 263.
6. Masuda, T., Kobayashi, T. and Toda, H., Submitted to *J. J. Inst. Light Met.*.
7. Yokoyama, T. (1996) *J. Soc. Mat. Sci*., 7, 785.
8. Mukai, T., Higashi, K., Tuchida, S. and Tanimura, S. (1993) *J. Inst. Light Met.,* 43, 252.